

# Structure and melting of blends of linear and branched polyethylenes crystallized at high undercooling

A. Alizadeh, A. Muñoz-Escalona\*, B. Vallejo and J. Martínez-Salazar†  
*Instituto de Estructura de la Materia, Serrano 119, 28006 Madrid, Spain; \*Repsol I + D,  
 Embajadores 184, 28045 Madrid, Spain*  
 (Received 20 July 1995; revised 27 May 1996)

A combined WAXD and d.s.c. study on blends of a series of commercial high density and low density (LD) polyethylene (PE) samples rapidly crystallized from the melt is presented. The melting curves of the materials are extensively analysed and compared to those exhibited by the individual components. The results, besides being indicative of a full compatibility of the two components, allow one to distinguish between a blend and an LDPE having both the same average value of branching. However, other structural parameters such as unit cell volume, macroscopic density or crystallinity, that are proved to be an exact average of the components, are unable to distinguish between the two materials. The result is applied to a series of commercial bimodal PEs. © 1997 Elsevier Science Ltd. All rights reserved.

(Keywords: polymer compatibility; lamellar distribution; crystallinity)

## INTRODUCTION

Blending of polyethylenes (PEs) with different branching contents has been traditionally used in order to improve the processability or the toughness of the resulting products<sup>1</sup>. A good example is the new kind of PE (Neste, Phillips, etc.) having bimodal molecular weight distribution. Indeed these bimodal PEs, which are generally produced either by melt or reaction blending<sup>2</sup> of high density (HD) and linear low density PE (LLDPE), show a noticeable improvement in processability as well as a better stiffness to toughness balance, together with a superior environmental stress cracking resistance<sup>3</sup>. For the optimization of the above properties a deep knowledge on the melt compatibility and final structure of the products is most desirable. Melt compatibility between ethylene segments having various degrees of pendant groups have been recently studied using model copolymers of hydrogenated polydienes<sup>4–7</sup> and LDPE and LLDPE<sup>8–12</sup>. All the results by direct methods such as small-angle neutron scattering point out a full compatibility for any two ethylene copolymers differing in less than 70–80 branches per 1000 carbons<sup>4–12</sup>. Let us call  $\epsilon_m$  this limiting value for compatibility. Above  $\epsilon_m$  there exists a critical behaviour which conforms to the predictions of the Flory–Huggins theory for random copolymers<sup>13</sup>. Melt compatibility clearly affects the microstructure of the semicrystalline blend. In fact, Barham and Hill<sup>14,15</sup>, based on microstructural studies of commercial HDPE and LDPE blends, have proposed a composition-based phase diagram with a close loop miscibility gap near the higher content of the branch component. However, the level of

branching of the LDPE or LLDPE used by these authors is much lower than  $\epsilon_m$ . To account for this discrepancy, in a recent paper, Mumby *et al.*<sup>16</sup> attempted to demonstrate that the degree of polydispersity in at least one of the components may induce the segregation of two PEs with a relative difference in branches lower than  $\epsilon_m$ .

In a previous study<sup>17,18</sup> carried out on different mixtures of HDPE and LDPE we reported a negative energy of mixing observed by melting point depression at 400 K whenever the branching content,  $\epsilon$ , was less than 25. The results, which were obtained by melting HDPE single crystals embedded in different amounts of LDPE, could be indicative of the behaviour of binary blends of polydisperse HDPE and LDPE, defining then a lower  $\epsilon_m$ . It was also postulated that the miscibility of the system could be due to the gain in entropy associated with the free volume excess created by the branches on mixing the polymers. The aim of this paper is to investigate the co-crystallization effects of various melt-compatible mixtures of HDPE and LDPE with  $\epsilon < 25$ . For them we have prepared blends of a series of high and low pressure Ziegler–Natta polymerized commercial PEs having different branching type and branching content. The extent of co-crystallization under quenching conditions similar to those employed in the manufacturing of pellets are analysed in terms of the melting curve distribution. Other parameters such as unit cell volume, enthalpy of fusion and macroscopic density are discussed. Bimodal PE samples from different producers are also included in this study. All the results are discussed in the light of previous LDPE data obtained in this laboratory. We are aware that the results presented in this paper may contradict other authors' results in PE blends as we believe that this type of result may depend on the molecular structure of both the linear and the

† To whom correspondence should be addressed

**Table 1** Molecular weight ( $M_w$ ), polydispersity index ( $M_w/M_n$ ) and branching content ( $\epsilon$ ) of the commercial PE samples

Sample name	Commercial name	$M_w \times 10^3$ (g mol <sup>-1</sup> )	$M_w/M_n$	$\epsilon$	Branch content (CH <sub>3</sub> /1000 C)			
					Me	Et	Bu	L,E <sup>a</sup>
					%			
H	Lupolen 6011L	159.0	12.2	1.1	—	—	—	100
A	Hostalen GF	144.0	13.4	7.0	20	46	—	34
B	Alkatene HD	207.0	10.9	9.3	—	—	50	50
C	Lupolen KR-1051	54.0	9.0	17.6	—	11	49	40
NES	Neste CPE-2594	313.7	15.6	7.0	—	47	—	53
HOS	Hostalen GM-5010	317.6	16.6	6.3	—	43	—	57
TUB	Tub-125	272.6	21.8	6.1	—	49	—	51

<sup>a</sup> Type of branching: Me, methyl; Et, ethyl; Bu, butyl; L,E, long chains and end groups

branched component. We have, therefore, made an effort to offer a full characterization of the samples at a molecular level.

## EXPERIMENTAL

### Materials characterization

The molecular weight,  $M_w$ , polydispersity index,  $n$ , and branching content,  $\epsilon$ , of the commercial PE samples used in this study are listed in *Table 1*. The bimodal samples present a very high  $n$  value of *ca* 16, as they are blends of high  $M_w$  LLDPE and low  $M_w$  linear PE. The total average values of branching,  $\epsilon$ , for each polymer expressed by the methyl content per thousand carbons are collected in *Table 1*. Previous sample characterization by i.r. spectroscopy<sup>19</sup> and a later characterization by <sup>13</sup>C nuclear magnetic resonance indicate that branches such as methyl, ethyl, butyl or longer chain sides are present in different amounts in the LDPE. The percentage value of each type of branch in each sample is also collected in the table. Since the bimodal PEs are reactor blends of linear and LLDPE from a butene comonomer, the branches are all ethyl type.

### Preparation of blends

Blends of the HDPE, H, and LDPEs A, B and C were prepared by dissolving both polymers in hot *p*-xylene followed by rapid precipitation and filtering. The compositions by weight of the (HDPE/LDPE) blends were: 0/100, 1/3, 1/1, 3/1 and 100/0. From now on, the blend made of HDPE, H, and LDPE, X, containing  $yy\%$  of the former will be designated as HX <sub>$yy$</sub> . In order to favour co-crystallization, all the samples were pressed into films 1 mm thick by melting them at 160°C and a nominal pressure of 150 bars for 5 min and rapidly crystallized by cooling to room temperature at a rate faster than 100°C min<sup>-1</sup>.

### D.s.c. measurements

The melting behaviour of the samples has been studied by differential scanning calorimetry (d.s.c.) using a Perkin Elmer DSC-7. To reduce possible differences among samples due to thermal lag during heat transfer across the sample pan, identical discoid samples of 100  $\mu$ m thickness and weight 2.4 mg were used. To detect any reorganization of the crystals during heating on the d.s.c. apparatus, the various melting endotherms were

recorded at heating rates of 10, 20 and 40°C min<sup>-1</sup>. Indium was used for temperature and specific heat calibration of the instrument while a paraffin fraction C<sub>32</sub>H<sub>66</sub> was used to correct the experimental curves for sample thermal lag.

### X-ray and macroscopic density measurements

Wide-angle X-ray diffraction experiments were performed at room temperature using a Rigaku X-ray powder diffractometer attached to a Rigaku generator with rotating copper anode operating at 40 kV and 140 mA. Nickel filtered  $K_\alpha$  radiation was detected by means of a scintillation counter equipped with a pulse-height analyser and discrimination units. The moulded samples having flat surfaces were carefully aligned on the diffractometer axis by means of a thin layer of silicon spread on to their surfaces. The positions of the different diffraction lines were corrected for sample absorption and thickness, slit divergence and sample planarity<sup>20</sup>. The 12 most intense reflections of PE in the Bragg interval  $10 \leq 2\theta \leq 50^\circ$  were analysed and the parameters of the orthorhombic unit cell were refined using least-squares fitting methods. The macroscopic densities of the samples were measured by means of a toluene/dioxane gradient column at 23°C.

## RESULTS AND DISCUSSION

### Melting behaviour of the blends

In *Figure 1* the experimental d.s.c. curves of all the studied samples are displayed. As a first observation, all the blends, irrespective of their relative concentrations except the HC25, exhibit a continuous single melting curve with no additional local maxima. The bimodal samples also show similar melting curves. The single melting distribution has been generally taken as a proof of co-crystallization in the sense that a single distribution of crystals containing both types of molecules, linear and branched, can be derived from it by using the Gibbs–Thomson relationship<sup>21,22</sup>. However, a close inspection of the curves reveals that there is indeed a progressive broadening of the curves as the concentration of LDPE,  $\phi$ , increases. Furthermore, neither the maximum nor the onset of the peaks seem to be substantially affected by the increasing value of  $\phi$  in each blend. As a consequence, the direct reading of those values may induce, as we shall demonstrate later on, meaningless results. Thus, in order

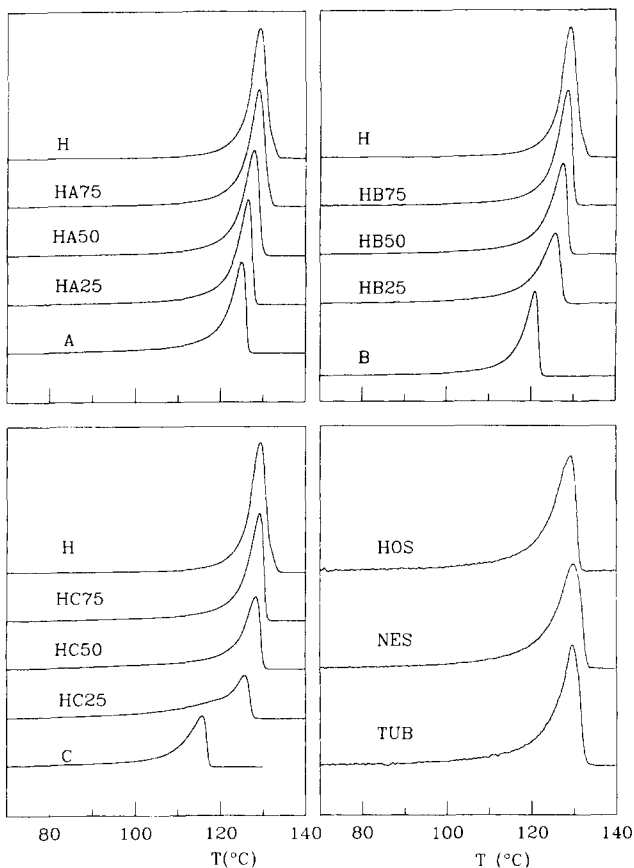


**Figure 1** Experimental d.s.c. melting curves of the blends HA, HB, HC and bimodal PE samples. Heating rate:  $10^{\circ}\text{C min}^{-1}$

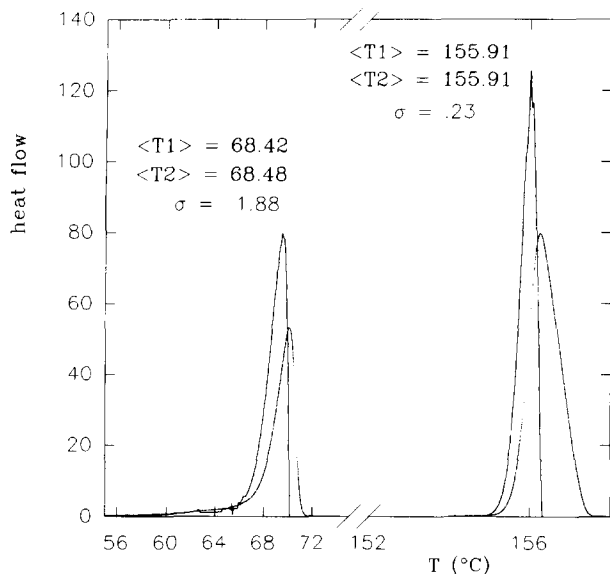


**Figure 2** Experimental and corrected melting curves for paraffin and indium standards. Heating rate:  $10^{\circ}\text{C min}^{-1}$ . See text for details of correction

to obtain more realistic and useful information about how the lamellar distribution and melting are modified in the blends in relation to their components it is necessary to establish a method of analysis which exceeds a simple and conventional evaluation of the curves. In the next two sections we will be first considering instrumental and sample effects' corrections followed by a comparative

description of the melting curves in terms of statistical parameters.

#### Corrections for thermal lag

It is well known that the melting curve of any substance in d.s.c. is distorted by instrumental factors<sup>23,24</sup>. Indeed, even pure substances having a sharp first order transition, i.e. an isothermal melting, are seen in d.s.c. as a relatively broad peak having an asymmetrical distribution of the melting curve around a maximum  $T_{\text{max}}$ . The two sides of the distribution, before and after  $T_{\text{max}}$  reflect the different responses of the system to heat absorption and heat dissipation. As far as our study is concerned we will restrict it to the former process, which in fact contains the total heat absorbed during the whole melting. Its time evolution depends on the rate of heat transference from the platinum platform to the melting front across the sample. Considering that instrumental factors are kept constant other factors such as sample thickness and sample resistivity are controlling the distribution of melting. Besides that, polymer crystals are known to have a distribution of crystal sizes that gives rise to a distribution of the melting characteristics of a non-isothermal process. Moreover, this distribution could be additionally modified during heating due to the instability of the lamellar crystals, which tend to thicken. Since all these effects are convoluted it is meaningless to derive a distribution of lamellar thickness by simply applying the Gibbs–Thomson relation to the experimental melting curves.

As an alternative to offering a framework of discussion we propose to analyse our melting data in terms of statistical terms such as the different momenta of the distribution and the partial areas from the accumulative curve. This latter point will be considered in the Discussion section. First, let us estimate the experimental broadening effects of the distribution due to the thermal resistance of the sample by using a paraffin fraction with identical geometry to the samples under study. *Figure 2* shows the melting curves of the paraffin  $\text{C}_{32}\text{H}_{66}$ . The melting of indium is also shown as a reference for instrument resolution. The broadening excess due to the delay in the heat transfer,  $-dq/dt$ , across the sample can be tentatively corrected according to the expression first proposed by Gray<sup>25</sup>:

$$\frac{dH}{dt} = \frac{-dq}{dt} + (C_s - C_r) \frac{dT}{dt} - RC_s \frac{d^2q}{dt^2} \quad (1)$$

where  $-dH/dt$  is the evolution of heat absorption by the sample per unit time,  $C_s$  and  $C_r$  are the heat capacities of the sample and reference, respectively, and  $R$  is the thermal resistivity of the sample. In order to evaluate the constant  $RC_s$ , the paraffin was recorded at different heating rates, keeping a constant sample thickness. From the expression:

$$T_{\text{true}} = T_{\text{exp}} - RC_s r \quad (2)$$

where  $T_{\text{true}}$  and  $T_{\text{exp}}$  are the correct and experimental  $T$  values, and  $r$  is the heating rate; a calculated value of 10 s for  $RC_s$  was obtained. The  $RC_s$  value for indium was taken as  $2.6 \text{ s}$ <sup>26</sup>. The heat absorptions for paraffin and indium were then corrected according to equation (1), and the results were plotted in *Figure 2*. The values of the first, moment  $\langle T^1 \rangle$ , and a second moment,  $\langle T^2 \rangle$ , as well as the standard deviation,  $\sigma$ , of both distributions are

included in the same figure. It is worthwhile noting that, while  $\langle T^1 \rangle$  and  $\langle T^2 \rangle$  differ for indium by  $0.001^\circ\text{C}$ , it is  $0.06^\circ\text{C}$  for the paraffin. The  $\sigma$  values are of the order of 0.23 and 1.88 for the indium and paraffin, respectively. These limiting values can be taken as representative of the instrument resolution, indium breadth, and sample resolution, paraffin breadth. The value of nearly  $2^\circ\text{C}$  for the paraffin could be considered high for an isothermal transition, but one has to take into account that the correction applied to  $dq/dt$  is based on a constant thermal resistance through the whole melting process, which is not strictly true. An excellent discussion on this topic can be found in the recent paper by Wang and Harrison<sup>27</sup>.

#### Analysis of the melting distribution curves by average values

As we have said above, the resolution in the melting of the lamellar crystals depends on the specific experimental setting. The experimental  $dq/dt$  curves have been corrected according to equation (1) to yield the  $dH/dt$  distribution. This distribution is now independent of the heating rate used. The width of the distribution is now reduced by a factor close to 30% and it is more representative of the lamellar distribution. The general appearance of the curves for most of the samples is still as of a single melting. *Figure 3* illustrates the results for HB25 and HC25. In the HC25 the initial shoulder is now much better resolved. Hence, the blend HC25 could be representative of the limiting values of branching and composition to observe a single melting curve. However, one has to bear in mind that since those values might depend on sample preparation and d.s.c. resolution the conclusion has to be considered under these limitations. In the HC25 we have tentatively separated the two melting distributions; each of them could be assigned to a distribution of lamellae population. The result yields a ratio between the two populations of 1/4.

In order to compare results from different series of blends it is convenient to define the average concentration of branches,  $\epsilon^*$ , in a given blend:

$$\epsilon^* = \epsilon \cdot \phi \quad (3)$$

where  $\epsilon$  and  $\phi$  are the branch content and the composition of the LDPE in the blend, respectively.

Let us now analyse in more detail the melting curve distribution of the samples. In *Figure 4* we have plotted the standard deviation,  $\sigma$ , as a function of  $\epsilon^*$  for the different blends after subtraction of the paraffin  $\sigma$  value. One can observe that the linear component has a  $\sigma$  value of 5.7 that is in all cases much lower than those corresponding to any of the LDPE component (8.0, 8.9 and 11.1 for A, B and C, respectively). The dotted lines are drawn joining the values of the constituents for each pair of blends. The HA blends show a nearly constant  $\sigma$  value close to the distribution of the A component. The HB blends exhibit a linear increase of  $\sigma$  up to a concentration of 50%, although the  $\sigma$  of the HB50 is slightly higher than that corresponding to the B component as it is also higher in the HB75. Similarly, the HC blends show a linear increase of  $\sigma$  as C is increased, but now the values are well above those corresponding to the C distribution. If one compares now the  $\sigma$  values as a function of  $\epsilon^*$  one observes that the four constituents can be situated on a single straight line. It is worthwhile mentioning that the increasing effect of broadening of the melting distribution

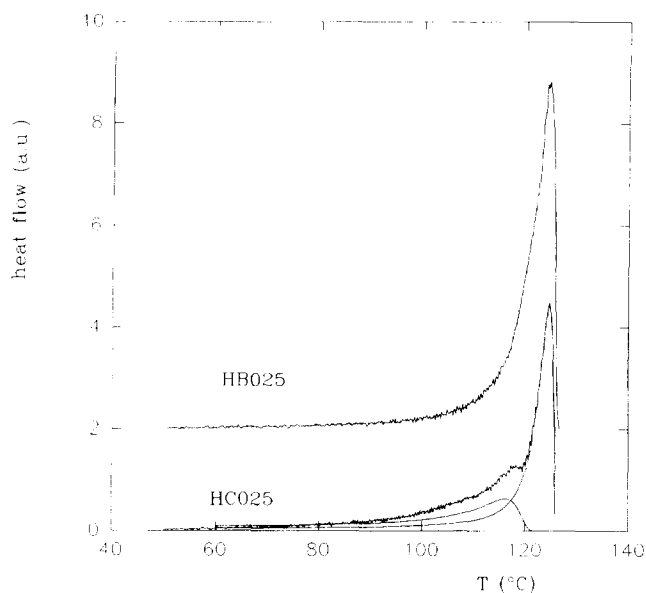


**Figure 3**  $dH/dt$  distribution for the blends HB25 and HC25. The separation of the two peaks in the HC25 is illustrated in the figure

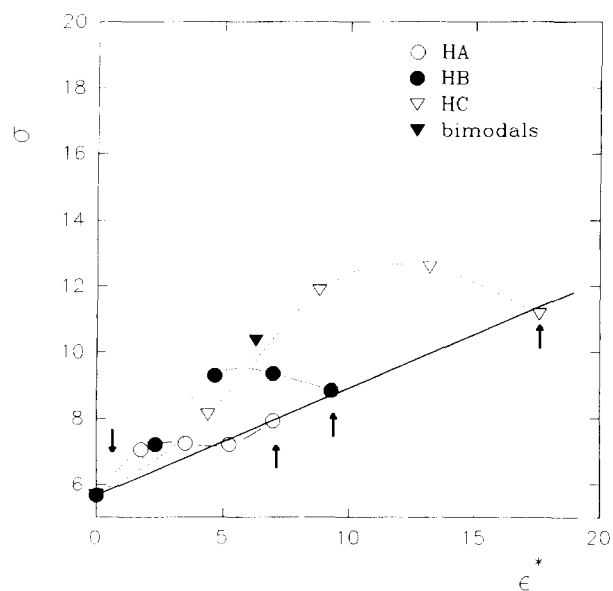


**Figure 4** Variation of the standard deviation,  $\sigma$ , of the corrected melting curves of the blends as a function of the average branching,  $\epsilon^*$ . The three bimodals have the same value

with increasing branching have been previously observed in these high pressure polymerized PEs<sup>28</sup>, although it has never been quantitatively described. Here, we have used our previously published data<sup>28</sup> to draw a master solid line in *Figure 4*.

We now observe that the blends are all above the master line as they are also the bimodal, so one can establish a clear distinction between an LDPE with a branching content  $\epsilon$  and a blend with an equivalent branching content  $\epsilon^*$ . Similarly, we have represented in *Figure 5* the mean value of the distribution,  $\langle T^1 \rangle$ , as a function of  $\epsilon^*$  for the different blends. Again, the average melting temperature for each blend is always higher than that corresponding to the linear interpolation of the respective components represented in the figure by the dotted lines. Naturally, the difference in temperature is

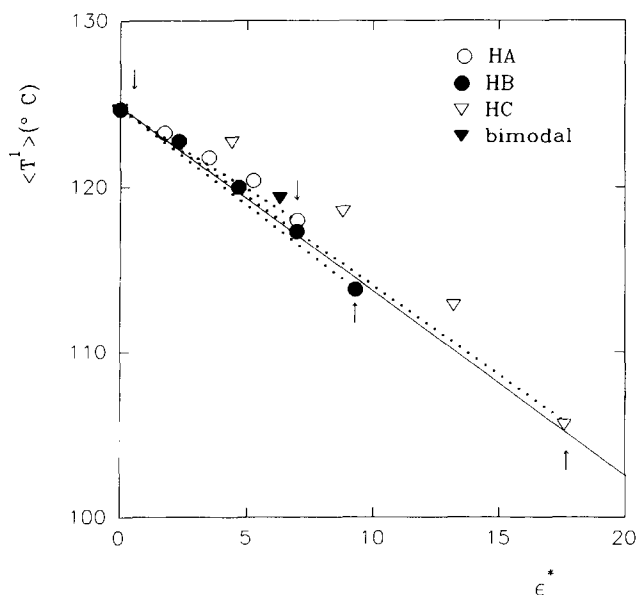


**Figure 5** Variation of the average temperature of melting of the corrected melting curves as a function of the average branching,  $\epsilon^*$ . Blends and bimodals are included

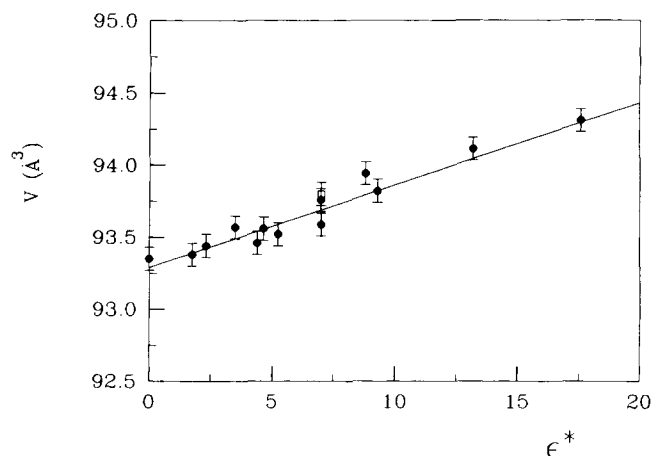


**Figure 6** Unit-cell volume as a function of the total branching content. The filled circles correspond to the HDPE/LDPE blends while the open symbols represent the bimodal samples

more significant as branching is increased. The linear decrease of the melting point with branching in LDPE crystallized under the same conditions was also previously observed by us in a series of LDPEs<sup>28</sup>. The linear tendency is marked in *Figure 5* with a solid master line. Again, one can establish a distinction between the LDPE and the equivalent blend by observing the first momentum of the distribution. The  $\langle T^1 \rangle$  of the three bimodals included in *Figure 5* clearly have melting values above the solid line, i.e. they behave as blends.

#### Unit cell expansion

The increase of the LDPE content in each blend results in an increase of the lattice parameters, particularly of the  $a$  axis. The  $c$  parameter, corresponding to twice the C–C bond projection along the molecular axis, remains approximately constant and equal to 2.547 Å. The variation of the unit cell volume as a function of  $\epsilon^*$  is plotted in *Figure 6*. The open symbols in this figure correspond to the bimodal samples. It can be observed

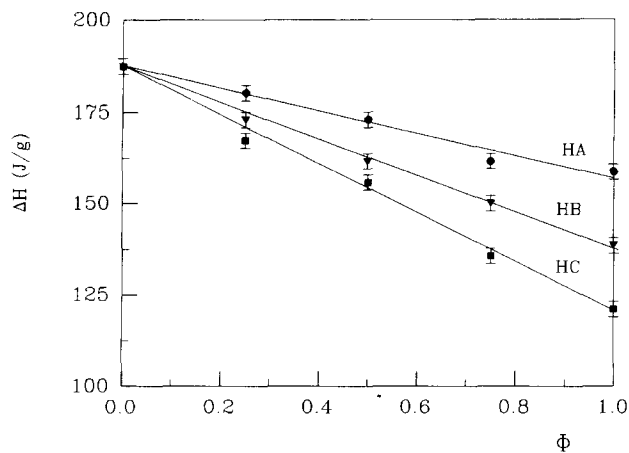


**Figure 7** Experimental enthalpy of fusion of the blends as a function of LDPE concentration,  $\phi$

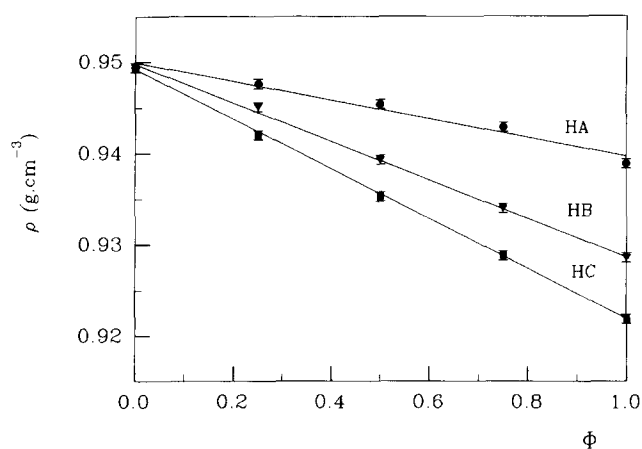


**Figure 8** Macroscopic density,  $\rho$ , as a function of LDPE concentration,  $\phi$ , for the different blends

that the individual components and their blends as well as the bimodal samples fit to the same line. Thus, the unit cell expansion is only a function of the total branching content, i.e. a blend with a total branch concentration  $\epsilon^*$  has the same cell dimensions as a pure polymer with identical branching content.

#### Enthalpy and macroscopic density

In *Figure 7* the variation of the enthalpy of fusion as a function of LDPE concentration for each series of blend is shown. It can be observed that the heat of fusion decreases almost linearly with  $\phi$ , and the slope becomes steeper with increase in the branching level of LDPE. In this case the enthalpy of fusion for a given blend is indeed an additive magnitude of its corresponding components. Similar results are found if one plots the macroscopic density as a function of LDPE concentration (see *Figure 8*). Again, a very well defined linear behaviour with concentration is obtained for each blend. For these two magnitudes it is useless to plot them as a function of an average  $\epsilon^*$  value since the variation of the crystallinity with branching has not been properly described yet.

## DISCUSSION

The blending of linear and branched PEs has received renewed interest since the polymerization of LLDPE in

the early 1980s. It was established soon after its commercial launch that the product was indeed a blend containing linear and branched molecules, the latter with a wide range of branching distribution<sup>29</sup>. In spite of the great effort made during the last few years to characterize properly the blend behaviour there are still fundamental points unsolved. The most prominent issue concerns segmental compatibility in the molten state. The second issue regards co-crystallization effects. While the first issue is relevant to blend preparation and processing the second issue affects the physical properties of the solidified products. It is clear that co-crystallization must involve compatibility, so by studying the solid state behaviour it is, in principle, possible to assess molecular compatibility in the molten state. In an effort to sketch the main answers to the above questions we have reviewed most of the recently published results on the melt compatibility of various LDPEs and LLDPEs. On the whole and leaving aside the different origins of the PE samples, one may assume that molecular compatibility between linear and branched PEs seems to occur whenever the overall branching content is < 20–30 per 1000 carbons<sup>11,30–34</sup>. The limiting value for branching is clearly lower than the one obtained by direct measurements in hydrogenated polybutadiene model copolymers<sup>4–7</sup>. This compatibility has been shown to exist for both long and short chain branching<sup>11,12</sup> and it does not seem to be very much affected by  $M_w$  distribution<sup>30</sup>. Our present results on the blends of commercial HDPE and LDPE and bimodal PE are clearly on this line, which are also confirmed by our previous published data on melting point depression<sup>17,18</sup>.

However, when trying to assess liquid–liquid phase separation from indirect methods such as d.s.c. melting curves one has to be cautious in the interpretation of co-crystallization. As we have said before the existence of a single melting curve has been taken as a proof of co-crystallization. Let us now analyse in more detail this concept. Strictly speaking co-crystallization means that two different molecules, in this case linear and branched PE, form part of the same lamella. This strong requirement is not absolutely necessary to account for melt compatibility. In fact nucleation effects, which also need a close molecular contact and hence liquid–liquid compatibility, may exist without co-crystallization. This nucleation effect, which surely alters the distribution of lamellae, could offer the apparent image of co-crystallization. The induced-crystallization, as we prefer to call this effect, will also give rise to an even morphological image when observed by electron microscopy<sup>14,15</sup>. On the other hand, to derive liquid–liquid phase separation from differentiated lamellar crystals is not a generally valid argument since segregation during crystallization is a very feasible situation in polymers. In any case if one admits partial co-crystallization it is necessary to establish a window of branching compatibility for two given molecules to co-exist in the same lamella.

According to our results induced crystallization of melt compatible HDPE and LDPE seems to occur under moderate conditions of cooling. The results clearly show that close molecular interaction does exist and molecular segments of branched and linear PE may coexist in some of the crystals as evidence by the unimodal distribution of melting curves. Unit cell, enthalpy of fusion and density seem to be an exact average of the two

components. In other words the structure of each individual polymer is transported to the blend. This is a very important point since one has to expect that a true co-crystallization should significantly modify the structural parameters. For instance, crystallinity should increase in the blend or the unit cell should be lower than the average value of the components. Nonetheless, some specific interactions between the two polymers are observed. This is particularly clear if one observes the distribution of lamellar populations. The melting curves provide a good framework of discussion on this point. As is well known the  $T_m$  data can be converted into crystal core thickness,  $l$ , by the well known Gibbs–Thomson equation [ $l = 2\sigma_c T_m^\circ / \Delta H^\circ (T_m^\circ - T_m)$ ]. Let us assume to help discussion that the equilibrium melting enthalpy,  $\Delta H^\circ$ , the surface free energy,  $\sigma_c$ , and the equilibrium melting temperature,  $T_m^\circ$ , are constant or have small variations for the different lamella populations. The width of the distribution of a given lamellar population,  $\Delta l$ , is then proportional to the width of the melting interval  $\Delta T$ .

Let us construct the accumulative function of melting for each sample in the range between 35 and 140°C and find the temperature,  $T_f$  at which a certain percentage fraction,  $f$ , of material is molten. The difference  $T_{f2} - T_{f1}$  defines a range of melting temperature which can be associated to a range of lamellae. Let us now consider four arbitrary regions of melting: region I,  $T_{90} - T_{75}$ ; region II,  $T_{75} - T_{50}$ ; region III,  $T_{50} - T_{25}$  and region IV,  $T_{25} - T_{10}$ . The width intervals of melting are plotted on the left-hand side of *Figure 9* for the different pairs of blends. Full lines correspond to the width interval of each component, and broken lines are the expected average values, while symbols are the experimental values. The average melting temperature for each interval of melting is plotted on the right-hand side of the figure as a function of  $\phi$ . Let us first concentrate on region I. This region is representative of the more perfect crystals. It is clear from data in *Figure 9* that the lamellae population characteristic of the HDPE maintains its distribution in each blend irrespective of the concentration. The small linear decrease of  $T_m$  with concentration can be explained by the gain in entropy during melting as we have mentioned earlier<sup>18</sup>. The  $T_m$  value can be resolved in branching at a concentration of 75% of LDPE. For other concentrations the results between different pairs of blend cannot be distinguished. In region II and for  $\phi$  values of 50 and 75%, it is clear that the width of the lamellar distribution increases as compared to the average values for the blends HB and HC while HA fits the average. As far as  $T_m$  is concerned one observes again a small linear decrease up to 50% of LDPE with no relevant variation in branching. However, at a concentration of 75%,  $T_m$  clearly shows detectable decreases of various degrees for the blends HB and HC and its value increases with branching. In region III except for the blend HA there is a large broadening of the interval which in some cases, as in samples HC50 and HC25, exceeds the value of the component C. On the other hand, the  $T_m$  values are the average of the components. Finally, in region IV, corresponding to the most imperfect crystals, there is an excess of broadening and what is more important the  $T_m$  values are below the average values of the components. After all this analysis the following picture emerges: (a) a certain fraction of the material, approximately 25%, is made of

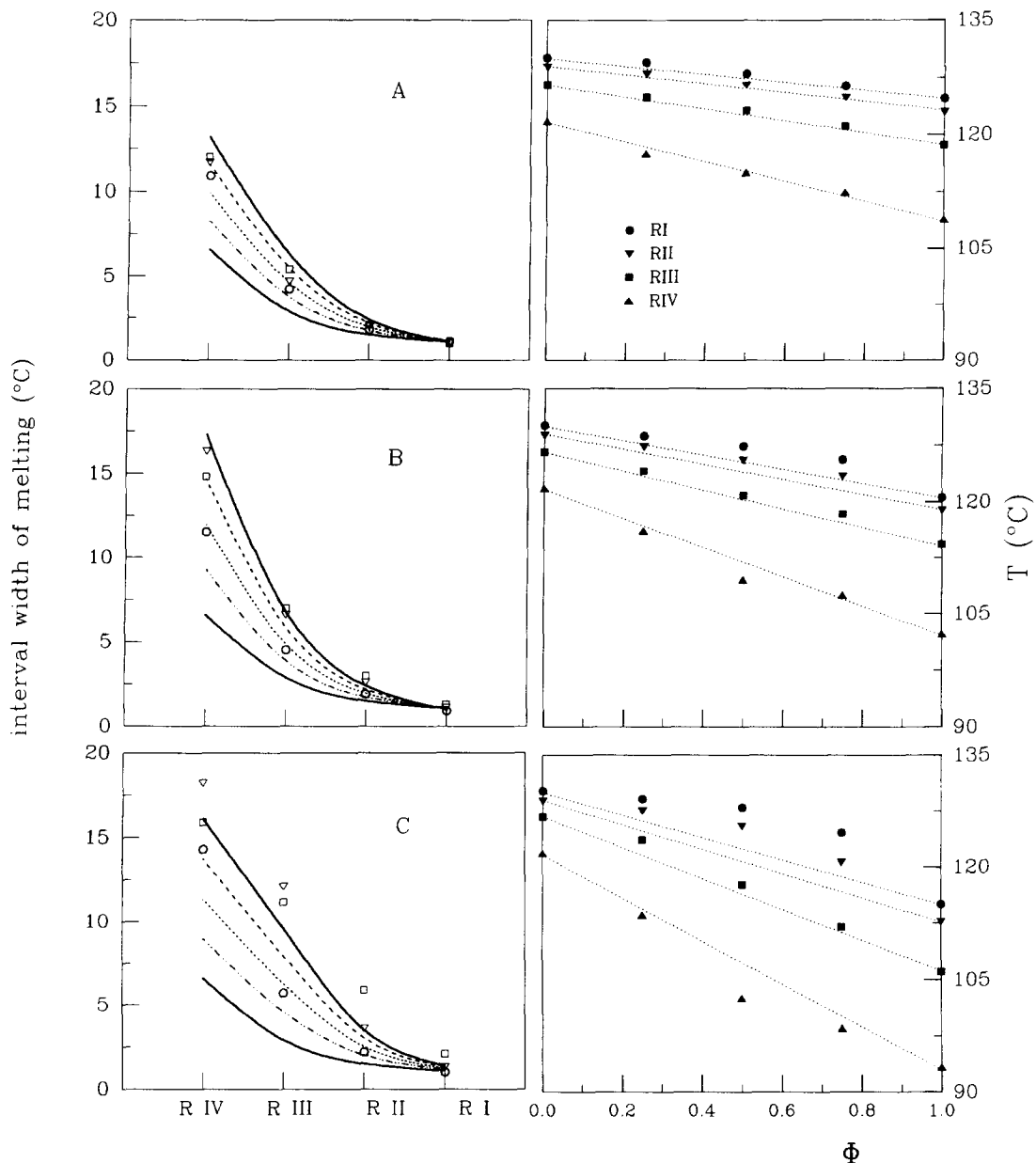


**Figure 9** On the left-hand side, width of melting; symbols, in four different regions of the melting curves and for different compositions: circles (3/1); squares (1/1); triangles (1/3). (A) Blend HA; (B) blend HB; (C) blend HC. The dotted lines are the average values calculated from the constituents. On the right-hand side, the corresponding average melting temperature in each region as a function of concentration. Symbols as indicated in the figure

crystals containing predominantly linear molecules; this population of crystals is independent of the blend type; (b) the linear molecules could co-crystallize with slightly branched PE molecules (*ca* seven branches per 1000 C as in case HA); (c) the process of crystallization seems to be enhanced by the linear molecules through nucleation, but the distribution of lamellar thickness is predominantly controlled by the branched polymer. This interaction results in a selective segregation of branched molecules imposed by the linear molecules during crystal nucleation.

The limiting value of  $\epsilon^*$  for observing a single melting distribution can be estimated around 15. A previous result on a 1/1 blend of HDPE with LDPE containing 30 branches/1000 C crystallized under the same conditions as the rest of the blends showed also partial segregation as revealed by d.s.c.<sup>35</sup> which is in accordance with the results obtained in this work. We have to emphasize

again that this late result does not imply a lack of compatibility in the melt. Similar objections could be applied to the results of Barham and Hill<sup>14,15</sup> who established a detailed and complex phase diagram based on solid state observations. In any case the above upper branching limit of 15 may be dependent on the type of branching and it could be well higher for smaller side groups. To conclude best defined answers on melt compatibility a more systematic study, based on neutron scattering experiments or rheological behaviour of the PE blends, is clearly needed.

The bimodal PEs, which have an average molecular weight of  $3 \times 10^5 \text{ g mol}^{-1}$ , follow the same trend as the HDPE/LDPE blends as has been demonstrated by the study of the different structural parameters. According to the g.p.c. evaluation<sup>36</sup> they behave as blends of unfractionated linear and branched PEs. Assuming that the branching content of the linear constituent of

the bimodal samples is negligible, the concentration of the branches for the branched component can be estimated to be between 10.5 and 15.7 per 1000 C, well inside the compatibility range and within the limits for single melting behaviour. The molecular compatibility shown by these bimodal samples seems to indicate that the difference in  $M_w$  is not very relevant as far as crystallization between linear and branched PEs is concerned.

## CONCLUSIONS

Our experiments on unfractionated HDPE/LDPE blends have shown that, under rapid crystallization conditions and for LDPE branching concentrations  $\epsilon < 20/1000$  C, a single melting distribution is observed. Surprisingly, the crystallinity of the constituents is literally transposed to the blends. However, the crystal population is altered by the interaction between the linear and branched molecules during crystallization. The result is a true molecular segregation among different lamellar crystals whose distribution increases as compared to the LDPE constituent. Consequently, by means of a close inspection of the melting distribution curve, it is possible to distinguish between a blend and an LDPE with the same average value of branching. A limiting value of branching to observe single melting could be situated around 15 branches per 1000 carbons. Care has to be taken to interpret deviations from single melting distribution as to be due to liquid-liquid phase separation. The three commercial bimodal PEs can be considered as blends of linear and branched PEs with approximately the same weight of each component. No significant influence of the molecular weight on the structural properties and melting have been found. Neither type of branches seems to alter the overall behaviour of the blends. This important fact allows a large versatility in designing new bimodal PEs by varying the molecular weight and the proportions of the linear and the branched components at a fixed total branching content  $\epsilon$ .

## ACKNOWLEDGEMENTS

We wish to thank the CICYT (grant MAT94-0825) and CAM (grant I + D 0094) for their kind support of this investigation.

## REFERENCES

- 1 Utraki, L. A. 'Polymer Alloys and Blends', Hanser Publishers, Munich, 1989
- 2 'Polyethylene Blends', Phillips Petroleum, *Eur. Patent 0533 155 A1*, 1993
- 3 Bohm, L. L., Enderle, H. F. and Fleissner, M. in 'Catalysts

- Design for Tailor Made Polyolefins' (Eds K. Soga and M. Terano), Koshdan, Tokyo, 1994
- 4 Nicolson, J. C., Finerman, T. M. and Crist, B. *Polymer* 1990, **31**, 2287
- 5 Rhee, J. and Crist, B. *Macromolecules* 1991, **24**, 5663
- 6 Balsara, N. P., Fetters, L. J., Hadjichristidis, N., Lohse, D. J., Han, C. C., Greassley, W. W. and Krishnamoorti, R. *Macromolecules* 1992, **25**, 6137
- 7 Krishnamoorti, R., Greassley, W. W., Balsara, N. P. and Lohse, D. J. *J. Chem. Phys.* 1994, **100**, 3894
- 8 Tashiro, K., Stein, R. and Hsu, S. L. *Macromolecules* 1992, **25**, 1801
- 9 Tashiro, K., Izuchi, M., Kobayashi, M. and Stein, R. *Macromolecules* 1994, **27**, 1221
- 10 Tashiro, K., Imanishi, K., Izumi, Y., Kobayashi, M., Kobayashi, K., Satoh, M. and Stein, R. *Macromolecules* 1995, **28**, 8477
- 11 Stehling, F. C. and Wignall, G. D. *Polym. Preprints (Am. Chem. Soc., Div. Polym. Chem.)* 1983, **24**, 211
- 12 Alamo, R. G., Londono, J. D., Mandelkern, L., Stehling, F. G. and Wignall, G. D. *Macromolecules* 1994, **27**, 411
- 13 Flory, P. J. 'Statistical Mechanics of Chain Molecules', Wiley Interscience, New York, 1969
- 14 Barham, P. J. in 'Materials Science and Technology. Structure and Properties of Polymers' (Ed. E. L. Thomas), Vol. 12, VCH, New York, 1993
- 15 Hill, M. J. and Barham, P. J. *Polymer* 1995, **36**, 1523
- 16 Mumby, S. J., Sher, P. and van Ruiten, J. *Polymer* 1995, **36**, 2921
- 17 Martínez-Salazar, J., Sánchez Cuesta, M. and Plans, J. *Polymer* 1991, **32**, 2984
- 18 Plans, J., Sánchez Cuesta, M. and Martínez-Salazar, J. *Polymer* 1991, **32**, 2989
- 19 Rueda, D. R., Baltá Calleja, F. J. and Hidalgo, A. *Spectrochim. Acta* 1979, **35A**, 847
- 20 Klug, H. P. and Alexander, L. 'X-Ray Diffraction Procedures for Polycrystalline and Amorphous Materials', Ch. 5. John Wiley, New York, 1974
- 21 Wunderlich, B. 'Macromolecular Physics', Vol. 2. Academic Press, New York, 1976, pp. 88-105
- 22 Rego López, J. M., Conde-Braña, M. T., Terselius, B. and Gedde, U. W. *Polymer* 1988, **29**, 1045
- 23 O'Neill, M. J. *Analyt. Chem.* 1964, **36**, 1236
- 24 Bershtein, V. A. and Ergov, V. M. 'Differential Scanning Calorimetry of Polymers. Physics, Chemistry, Analysis, Technology', Ellis Horwood, Chichester, UK, 1994
- 25 Gray, A. 'Analytical Calorimetry', Vol. 1, Plenum Press, New York, 1976, p. 322
- 26 Manual of Perkin-Elmer, DSC-4 Instructions, pp. 3-27
- 27 Wang, G. and Harrison, I. R. *Thermochim. Acta* 1994, **231**, 203
- 28 Martínez-Salazar, J., Sánchez Cuesta, M. and Baltá Calleja, F. J. *Colloid Polym. Sci.* 1987, **265**, 239
- 29 Mathot, V. B. F. and Pijpers, M. J. F. *J. Appl. Polym. Sci.* 1990, **39**, 979
- 30 Alamo, R. G., Glaser, R. H. and Mandelkern, L. *J. Polym. Sci.: Polym. Phys.* 1988, **26**, 2169
- 31 Alamo, R. G. and Mandelkern, L. *Polym. Preprints* 1992, **33**, 1208
- 32 Conde-Braña, M. T., Irigorri-Sainz, J. I., Terselius, B. and Gedde, U. W. *Polymer* 1989, **30**, 410
- 33 Irigorri, J. I., Rego, J. M., Katima, I., Conde-Braña, M. T. and Gedde, U. W. *Polymer* 1992, **33**, 461
- 34 Alamo, R. G. and Mandelkern, L. *Polym. Preprints* 1995, **36**, 136
- 35 Sánchez Cuesta, M. Ph. D. Dissertation, University Complutense of Madrid, 1992
- 36 Alizadeh, A., Muñoz-Escalona, A. and Martínez-Salazar, J. *Polym. Eng. Sci.* (submitted)